Bioorganic Chemistry 87 (2019) 857–866

Contents lists available at ScienceDirect

Bioorganic Chemistry

journal homepage: www.elsevier.com/locate/bioorg

Benzoxazinone-thiosemicarbazones as antidiabetic leads *via* aldose reductase inhibition: Synthesis, biological screening and molecular docking study

Muhammad Tariq Shehzad[a], Aqeel Imran[b], Guy Sedar Singor Njateng[b], Abdul Hameed[c], Muhammad Islam[a], Mariya al-Rashida[d], Maliha Uroos[e], Asnuzilawati Asari[f], Zahid Shafiq[a,*], Jamshed Iqbal[b,*]

[a] Institute of Chemical Sciences, Bahauddin Zakariya University, Multan 60800, Pakistan
[b] Centre for Advanced Drug Research, COMSATS University Islamabad, Abbottabad Campus, Abbottabad 22060, Pakistan
[c] H.E.J. Research Institute of Chemistry, International Center for Chemical and Biological Sciences, University of Karachi, Karachi 75270, Pakistan
[d] Department of Chemistry, Forman Christian College (A Chartered University), Ferozepur Road, Lahore 54600, Pakistan
[e] Institute of Chemistry, University of Punjab, Lahore, Pakistan
[f] School of Fundamental Science, Universiti Malaysia Terengganu, 21030 Kuala Terengganu, Terengganu, Malaysia

ARTICLE INFO

Keywords:
Aldose reductase
Benzoxazinone
Thiosemicarbazones
Molecular docking

ABSTRACT

Aldose reductase is an important enzyme in the polyol pathway, where glucose is converted to fructose, and sorbitol is released. Aldose reductase activity increases in diabetes as the glucose levels increase, resulting in increased sorbitol production. Sorbitol, being less cell permeable tends to accumulate in tissues such as eye lenses, peripheral nerves and glomerulus that are not insulin sensitive. This excessive build-up of sorbitol is responsible for diabetes associated complications such as retinopathy and neuropathy. In continuation of our interest to design and discover potent inhibitors of aldo-keto reductases (AKRs; aldehyde reductase ALR1 or AKR1A, and aldose reductase ALR2 or AKR1B), herein we designed and investigated a series of new benzoxazinone-thiosemicarbazones **(3a-r)** as ALR2 and ALR1 inhibitors. Most compounds exhibited excellent inhibitory activities with IC_{50} values in lower micro-molar range. Compounds **3b** and **3l** were found to be most active ALR2 inhibitors with IC_{50} values of 0.52 ± 0.04 and 0.19 ± 0.03 μM, respectively, both compounds were more effective inhibitors as compared to the standard ALR2 inhibitor (sorbinil, with IC_{50} value of 3.14 ± 0.02 μM).

1. Introduction

Taking into account its increasing prevalence of diabetes mellitus (DM), it is speculated that it may become world's largest public health issue in the coming decades. According to an estimate, the number of people suffering from DM exceeded over 400 million by the year 2015, and by 2040 this number is predicted to increase to 642 million [1,2]. The close epidemiological resemblance of DM (mainly type 2) and cancer further increases the risk of developing various cancer types in diabetic patients. The hyperglycemia in DM leads to chronic diabetic complications including nephropathy, mood disorders, neuropathy and retinopathy whereas the abnormal polyol pathway flux is included amongst the secondary diabetic complications [3–5] (see Scheme 1).

The polyol pathway involves the glucose metabolism, and in hyperglycemic conditions in the non-insulin dependent cells [3], this polyol pathway is activated to metabolize the excess glucose resulting in devastating effects with increased advanced glycation end products (AGEs), protein kinase C (PKC), mitogen activated protein kinase (MAPK), reductive, oxidative and glycative stress [6–8]. The aldose reductase (ALR2, EC 1.1.1.21) is a monomeric oxidoreductase enzyme involved in polyol pathway for the reduction of various carbonyl compounds particularly glucose to sorbitol *via* co-factor NADPH. Sorbitol is then converted to fructose by sorbitol dehydrogenase utilizing the co-factor NAD^+. The poor penetration of sorbitol and its further metabolism significantly increases the polyol flux. Under normoglycemic condition, the glucose is transformed into glucose-6-phosphate via glycolytic pathway, whereas under hyperglycemia, the capacity of ALR2 to bind to glucose enhances dramatically leading to various complications including glaucoma and cataract due to excessive sorbitol accumulation [9,10]. Thus development of efficient and selective

* Corresponding authors.
E-mail addresses: zahidshafiq@bzu.edu.pk (Z. Shafiq), drjamshed@ciit.net.pk (J. Iqbal).

https://doi.org/10.1016/j.bioorg.2018.12.006
Received 30 October 2018; Received in revised form 3 December 2018; Accepted 3 December 2018
Available online 11 December 2018
0045-2068/

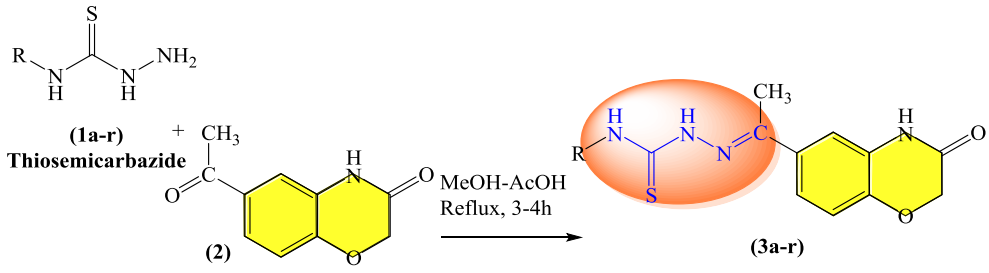

R = Subsitutents

(a)	R = C_6H_5	**(k)**	R = 2-FC_6H_4
(b)	R = 3-BrC_6H_4	**(l)**	R = 3-FC_6H_4
(c)	R = 3-ClC_6H_4	**(m)**	R = 4-$NO_2C_6H_4$
(d)	R = $C_6H_5CH_2$	**(n)**	R = H
(e)	R= 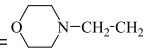	**(o)**	R = 4-FC_6H_4
(f)	R= 2-$ClC_6H_5CH_2$	**(p)**	R = 2,4-$(Cl)_2C_6H_3$
(g)	R= $C_{10}H_7$	**(q)**	R= 2,6-$(CH_3)_2C_6H_3$
(h)	R= 3-$OCH_3C_6H_4$	**(r)**	R = 2-$CH_3C_6H_4$
(i)	R = 4-$CH_3C_6H_4$		
(j)	R = C_6H_{11}		

Scheme 1. Synthesis of benzoxazinone derived thiosemicarbazones **(3a-r)**.

ALR2 inhibitors is a potential target to mitigate the complications of diabetes.

One of the main impediments in developing ALR2 inhibitors is the concomitant inhibition of a related enzyme Aldehyde Reductase (ALR1, EC 1.1.1.2), which is responsible for the metabolism of toxic aldehyde intermediates like 3-deoxyglucosone and methyl glyoxal. Both ALR1 and ALR2 belong to the same aldo-keto reductase (AKR) superfamily and hence share 65% structural homology [11]. Although various natural and synthetic aldose reductase inhibitors (ARIs) have been evaluated for both *in vivo* and *in vitro* screening [12–15], Epalrestat is the only marketed drug by ONO Pharmaceutical, Japan [16,17]. Amongst synthetic ARIs, the majority of them entering clinical trials are either hydantoins or carboxylic acid derivatives, which suffer from extreme pharmacokinetic drawbacks due to their adverse side effects and non-selectivity [11,17]. Therefore, to control and mitigate chronic diabetic complications through suppression of polyol pathway, the development of selective ALR2 inhibitors is vital. There are various molecules that have been explored as ALR2 inhibitors [18]. In our research, we have synthesized, and studied several (thio)semicarbazones, and found them to be highly biologically active molecules [19–21]. Some other groups have also explored the therapeutic potential of thiosemicarbazones [22–26]. This led us to explore the use of this (thio) semicarbazone pharmacophore, coupled with benzoxazinone ring as inhibitors of both ALR1 and ALR2.

2. Results and discussion

2.1. Chemistry

To explore the potential of benzoxazinone derived thiosemicarbazones (**3a-r**), a series of - substituted thiosemicarbazones (**TSC**) were prepared. A typical condensation method was used by reacting thiosemicarbazides (**1a-r**) with 6-acetyl-2*H*-benzo[*b*][1,4]oxazin-3(4*H*)-one (**1**). The reaction was carried out in methanol under the catalysis of glacial acetic acid (1–2 drops). The optimization of reaction conditions was done by treating equimolar amounts of phenyl thiosemicarbazide (**1a**) and 6-acetyl-2*H*-benzo[*b*][1,4]oxazin-3(4*H*)-one (**1**) in the presence of solvents of mutable polarity i.e. methanol, DMSO, ethanol, THF and DCM. The optimum conditions were established by carrying the reaction under reflux in methanol as solvent and by using glacial acetic acid as a catalyst. The scope of reaction was extended by employing a range of thiosemicarbazides (**1a-r**). The targeted thiosemicarbazones (**3a-r**) were obtained in good to excellent yields (70–91%).

The structures of benzoxazinone hybrids of thiosemicarbazides (**3a-r**) were established using microanalysis (CHN) and spectral data i.e. IR, ^{1}H NMR, ^{13}C NMR. The C═N band in FTIR appeared in the range of 1518–1596 cm^{-1} while C═S appeared in the range from 1169 to 1281 cm^{-1}. NH− appeared stretching from 3127 to 3485 cm^{-1} and C═O band was observed between 1666 and 1703 cm^{-1}. In ^{1}H NMR, O−CH2− signal appeared as singlet in the range from δ 4.55–4.82 ppm while the NH−C═S, NH−N and NH−C═O were observed as broad singlet ranging from δ 8.29–10.24, 10.32–10.74 and 10.66–11.00 ppm respectively. The spectral data of other aromatic and aliphatic protons was also in accordance with the structures of anticipated compounds. CHN analysis also supported the anticipated structures (**3a-r**) and the observed values were in good agreement with the values found (see Fig. 1).

2.2. Bioactivity (in vitro enzyme inhibition)

The inhibitory activity of benzoxazinone derived thiosemicarbazones **(3a-r)** series was tested *in vitro* against both aldose reductase (ALR2) and aldehyde reductase (ALR1). Compound **3n** with free NH_2 group showed weak inhibitory activity (21.9%) against aldose reductase (ALR2), as well as against aldehyde reductase (7.42%). However, functionalization of NH_2 group with different substituents was found to enhance the inhibitory activity of most of the benzoxazinone derived thiosemicarbazones **(3a-r)** (Table 1). The phenyl substituted benzoxazinone-thiosemicarbazone **(3a)** showed excellent inhibitory activity against ALR2 with IC_{50} value of 1.84 ± 0.01 μM, and comparatively less inhibitory against ALR1 (IC_{50} = 6.76 ± 0.63 μM). The presence of benzyl group in compound **3d** reduced the inhibitory activity against ALR2 (IC_{50} = 23.1 ± 1.22 μM) (Fig. 2).

The inhibition of ALR2 with halogen substituted benzoxazinone-

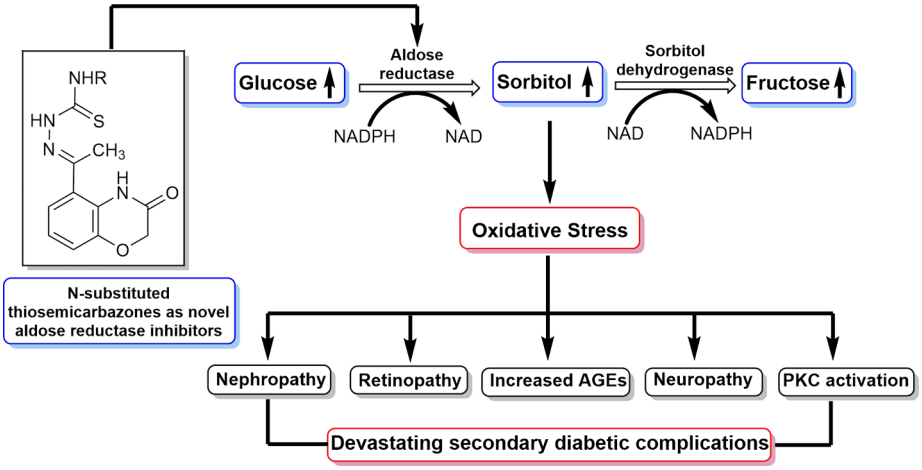

Fig. 1. Mechanism of polyol pathway.

thiosemicarbazones showed varied activity with IC_{50} values ranging from 0.19 ± 0.03 to 19.8 ± 1.90 μM. The 3-bromophenyl containing compound **3b,** and 3-fluorophenyl substituted thiosemicarbazones **3l** showed excellent ALR2 inhibitory activities with IC_{50} values of 0.52 ± 0.04 and 0.19 ± 0.03 μM respectively, as compared to the standard inhibitor sorbinil (IC_{50} = 3.14 ± 0.02 μM). Compound **3b** was found to be about 35 times more active against ALR2 as compared to ALR1 (**3b**; ALR1 IC_{50} = 18.3 ± 0.32), whereas compound **3l** was only moderately more active (about 9 times) against ALR2 as compared to ALR1 (ALR1 IC_{50} = 1.72 ± 0.02 μM). Both compounds (**3b** and **3l**), were more active ALR1 inhibitors than the standard inhibitor valproic acid (IC_{50} = 57.4 ± 0.89 μM). The 3-chlorophenyl substituted compound **3c** (IC_{50} = 10.6 ± 1.14 μM), and 3-chlorobenzyl substituted compound **3f** (% inhibition = 10.8%) showed comparatively less ALR2 inhibitory activity (Fig. 3). In case of fluoro substituent, the ALR2 inhibitory activity of 2-fluorophenyl containing compound **3k**, and 4-fluorophenyl containing compound **3l** decreased further (% inhibition = 19.8% and 19.3%, respectively). The 2,3-dilchlorophenyl substituted thiosemicarbazone **3p** exhibited somewhat increased ALR2 inhibitory activity (IC_{50} = 2.34 ± 0.03 μM), however it was still lower than the standardard sorbinil (Fig. 4).

Compound **3m,** having electron withdrawing group/substutuent (4-nitrophenyl) showed weak inhibitory activity against ALR2 (IC_{50} = value of 0.19 ± 0.03 μM and non-active (12.7% inhibition). The compound **3m** showed high selectively for ALR2. Further the thiosemicarbazones bearing non-aromatic rings *i.e.* morpholinyl **3e** and cyclohexyl **3j** showed low percentage inhibition values for ALR2. Both can be considered as non-active for ALR2 inhibition (Fig. 4).

The compounds **(3g, 3h, 3i, 3q,** and **3r)** with naphthyl, methyl, methoxy showed weak inhibition activity for ALR2 (% inhibition = 10.9%, 19.3%, 23.1%, 12.0%, and 17.3%, respectively) (Fig. 5). Compounds 3g and 3q showed excellent ALR1 inhibitory activity (3g: IC_{50} = 5.81 ± 0.12 μM; 3q: IC_{50} = 1.53 ± 0.21 μM), whereas compound 3r showed moderate ALR1 inhibition activity (C_{50} = 30.4 ± 0.73 μM).

2.3. Docking results

The experimental results revealed that compound **3b** was selective inhibitor of aldose reductase (ALR2), whereas **3s** was selective inhibitor of aldehyde reductase (ALR1). The compound exhibiting dual inhibition against both the enzymes was **3l**, as it showed significant inhibition against aldose reductase along with good inhibitory activity against aldehyde reductase. Therefore the docking studies for all these compounds were carried out. The inhibitors selected for docking against ALR2 were **3b** and **3l** whereas, **3q** and **3l** were docked against ALR1.

For carrying out docking analysis, the protein structures were downloaded from the Protein Data Bank. In case of aldose reductase (ALR2), the crystal structure of human ALR2 was available [PDB id: 1US0, at 0.66 Å] [27] and was downloaded. However, human aldehyde reductase crystal structure was not available, therefore porcine aldehyde reductase [PDB id: 3FX4, at 1.85 Å] was selected [28,29].

Prior to docking with synthesized compounds, method validation was carried out by re-docking the inhibitor (LDT320) that had co-crystallized with hALR2 enzyme. The docking software (LeadIT) [30] was able to reproduce the experimentally observed conformation of the co-crystallized inhibitor with rmsd of 0.69 Å. Two most active ALR2 inhibitors, 3 l, and 3b were selected for docking studies. All compounds were found in the same area of the active site as that of co-crystallized inhibitor LDT320, with similar binding orientations and interaction. Fig. 6 shows overlap of docked ALR2 inhibitors with the co-crystallized inhibitor LDT320.

All compounds were found to have similar binding site interactions. Fig. 7 shows 3D and 2D docked conformations of compounds **3b** and **3l**. For compounds **3b** and **3l**, the oxygen atom of the carbonyl group was making hydrogen bond interactions with Tyr48 and His110, while one of the amino groups (=N–NH–) was making hydrogen bond with Ala299. The benzene ring of benzoxazinone ring was making pi-stacked interactions with Trp20 and Trp219, while the phenyl ring was also making pi-stacked interaction with Trp219.

For ALR1 docking, method validation was similarly carried out by re-docking the inhibitor (FID2401) that had co-crystallized with the ALR1 enzyme. The docking software reproduced the experimentally observed conformation of the co-crystallized inhibitor with rmsd of 0.69 Å. Two most active ALR1 inhibitors **3l**, and **3q** were selected for docking studies. All compounds were found to bind in the same area of the active site as that of co-crystallized inhibitor FID2401, with similar binding orientations and interactions. Fig. 8 shows overlap of docked ALR1 inhibitors with the co-crystallized inhibitor FID2401.

Both compounds, **3l** and **3q** were found to have similar binding site interactions. Fig. 9 shows 3D and 2D docked conformations of compounds **3l** and **3q** respectively. For compound **3q**, the ring oxygen atom was making hydrogen bond with Trp114, while the oxygen atom of the carbonyl group was making hydrogen bond with Tyr50. These two interactions were also observed for docked conformation of **3l**. The –NH group of compound **3q** was making hydrogen bond with Met302, while the azomethine nitrogen atom (=N–) of **3l** was making hydrogen bond with Trp22. For compound **3q**, an additional pi-stacked interaction was observed between the fused benzene ring of benzoxazinone scaffold and Trp82.

For ALR1 and ALR2 inhibitors, from the results of docking studies, the main pharmacopore responsible for activity seems to be, (i) a

Table 1
In vitro aldose reductase and aldehyde reductase inhibitory activities of compounds **3a-r**.

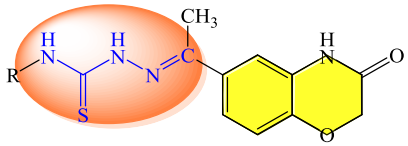

(3a-r)

Codes	Structures	ALR1	ALR2
		IC_{50} ± SEM (μM)[a]/%inhibition	
3a		6.76 ± 0.63	1.84 ± 0.01
3b	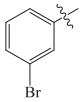	18.3 ± 0.32	0.52 ± 0.04
3c	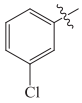	7.01 ± 0.21	10.6 ± 1.14
3d	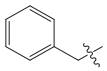	15.3%	23.1%
3e	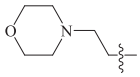	2.56%	20.2%
3f	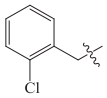	4.51 ± 0.30	10.8%
3g	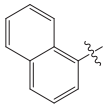	5.81 ± 0.12	10.9%
3h	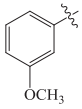	20.2%	19.3%
3i	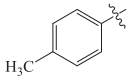	23.1%	23.1%
3j		7.11 ± 0.20	18.2%
3k	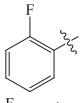	1.91 ± 0.01	19.8%
3l	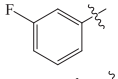	1.72 ± 0.02	0.19 ± 0.03
3m	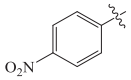	12.7%	3.91 ± 0.36
3n	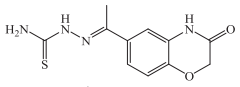	7.42%	21.9%
3o	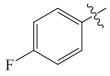	8.61 ± 0.15	19.3%
3p	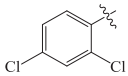	7.69%	2.34 ± 0.03

Table 1 (*continued*)

Codes	Structures	ALR1	ALR2
		IC_{50} ± SEM (μM)[a]/%inhibition	
3q	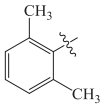	1.53 ± 0.21	12.0%
3r	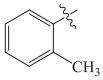	30.4 ± 0.73	17.3%
Valproic acid[b]	–	57.4 ± 0.89	–
Sorbinil[b]	–	–	3.14 ± 0.02

[a] Half maximal inhibitory concentration.
[b] Standard inhibitor.

hydrogen bond acceptor (a carbonyl group, in these compounds) substituted at the carbon atom adjacent to the NH group of benzoxazinone ring, and (ii) the thiourea (−N═NH−CO−NH−) linking group. For ALR1 inhibitors, additionally the oxygen atom (hydrogen bond acceptor) of the benzoxazinone ring is also an important pharmacophoric feature.

3. Conclusions

In conclusion, the biological screening of new benzoxazinone based thiosemicarbazones **(3a-r)** showed potent molecules to serve as potential leads for long-term diabetic complications *via* inhibition of aldose reductase ALR2. The compounds **3b** and **3l** were identified as potential leads as ALR2 inhibitors with IC_{50} values of 0.52 ± 0.04 and 0.19 ± 0.03 μM, respectively. The thiosemicarbazone **3b** (IC_{50} = 18.3 ± 0.02 μM for ALR1) showed high selectivity towards ALR2 to serve as lead for antidiabetic agents development. Moreover, the docking studies were carried out against the selective inhibitors of ALR1 and ALR2 as well as dual inhibitor presenting significant inhibition against both the enzymes.

4. Experimental work

4.1. Materials and methods

All the starting materials were purchased from different chemical supplies and used without purification. The thin layer chromatography (TLC) coated with silica gel 60 aluminium-backed plates 0.063–0.200 mm with suitable solvent systems as eluent to monitored the reactions. The UV light with 254 nm was used to visualize the TLC spots. The infrared spectra IR (KBr discs) were recorded in the range 4000–500 cm^{-1} *via* Bruker Vector-22 spectrometer. ^1H NMR spectra were recorded *via* Bruker spectrometer 300, 400 MHz as dilute solutions in suitable deuterated solvent at 25 °C. The chemical shifts were recorded on the *δ*-scale (ppm) using residual solvents as an internal standard (DMSO; ^1H 2.50, and $CHCl_3$; ^1H 7.26,). Coupling constant were calculated in Hertz (Hz) and multiplicities were labelled as s (singlet), d (doublet), t (triplet), q (quartet), quint (quintet) and the prefixes br (broad) or app (apparent) were used. Mass spectra (EI+) were recorded at Finnigan MAT-321A, Germany. Melting points of synthesized compounds were determined by means of a Stuart™ melting point SMP3 apparatus.

4.2. Chemistry

4.2.1. General procedure for the synthesis of compounds (3a-3r)

To a hot stirred solution of 6-acetyl-2*H*-benzo[*b*][1,4]oxazin-3(4*H*)-one (0.005 mol) **(2)** in methanol (10 mL) containing 1–2 drops of

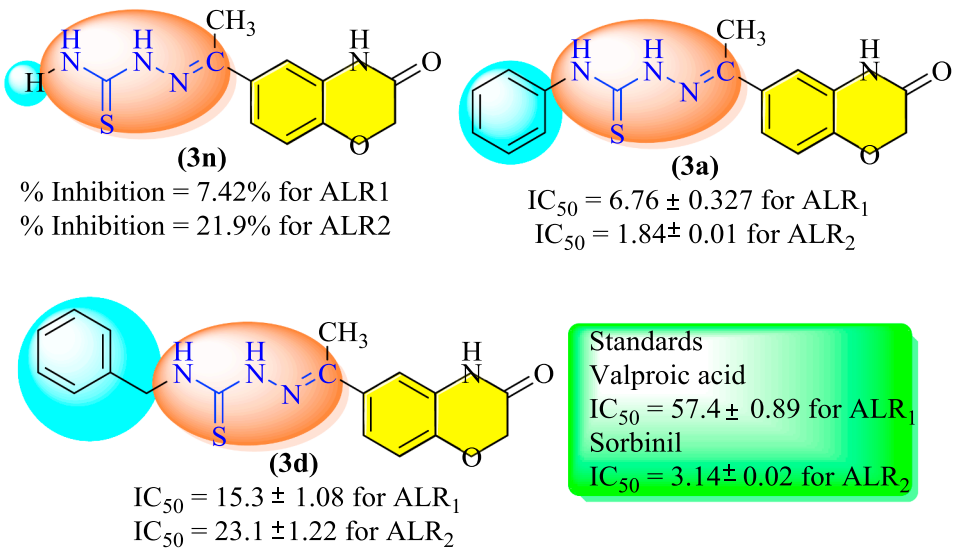

Fig. 2. Inhibitory activity of compounds **3n**, **3a** and **3d**.

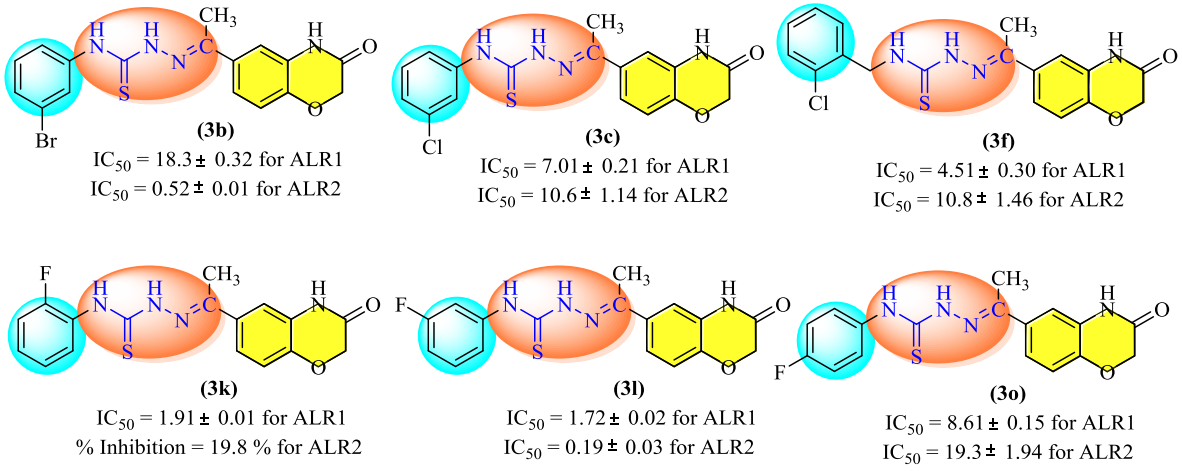

Fig. 3. Aldose reductase inhibitory activity of compounds **3b**, **3c**, **3f**, **3k**, **3l**, and **3o**.

glacial acetic acid as catalyst was added appropriate thiosemicarbazide (0.005 mol) **(1a-r)** dissolved in methanol (10 mL). The reaction mixture was then refluxed for 3–4 h and the completion of reaction was monitored through TLC. The crystalline solid formed during refluxing was collected by suction filtration. Thorough washing with cold methanol, followed by ether afforded the desired compounds **(3a-r)** which were recrystallized from ethanol.

4.2.1.1. 2-(1-(3-Oxo-3,4-dihydro-2H-benzo[b][1,4]oxazin-6-yl) ethylidene)-N-phenyl hydrazine carbothioamide (3a). Yield 82%, m.p.

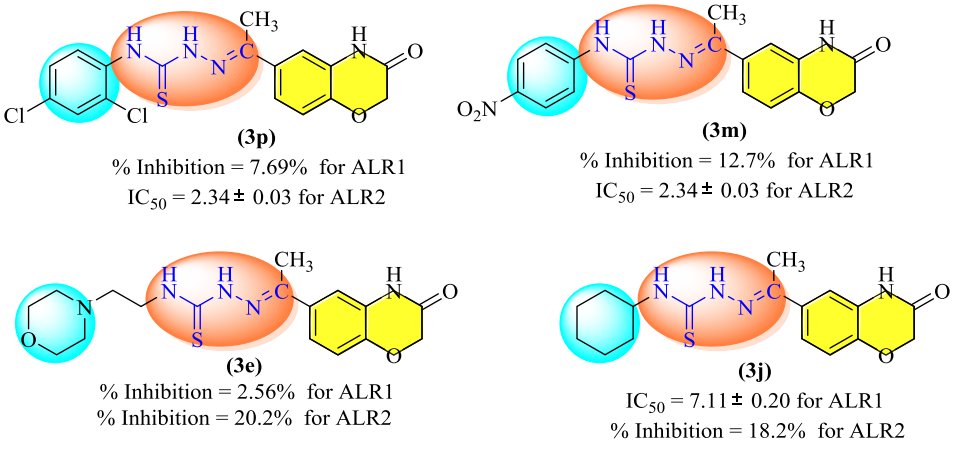

Fig. 4. Aldose reductase inhibitory activity of compound **3p**, **3e**, and **3j**.

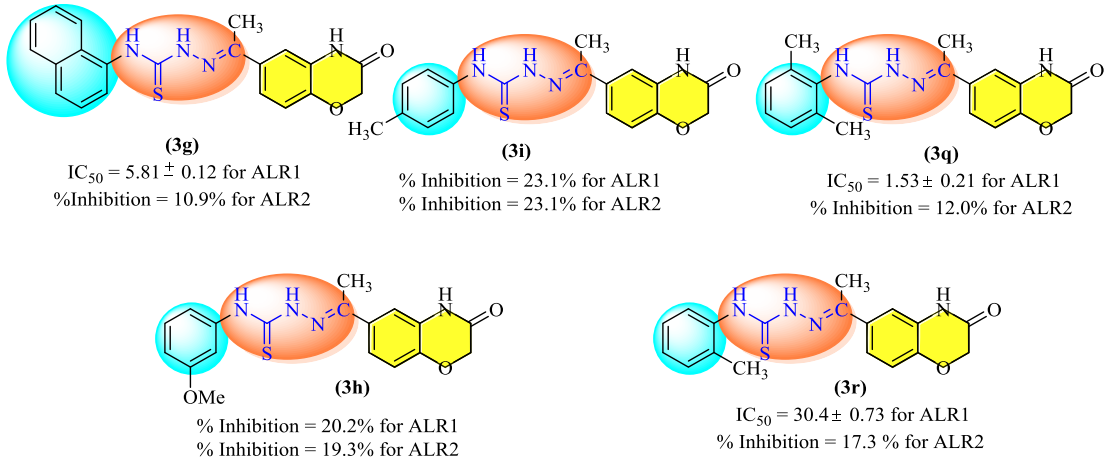

Fig. 5. Aldose reductase and aldehyde reductase inhibitory activity of compounds **3g, 3h, 3i, 3q and 3r.**

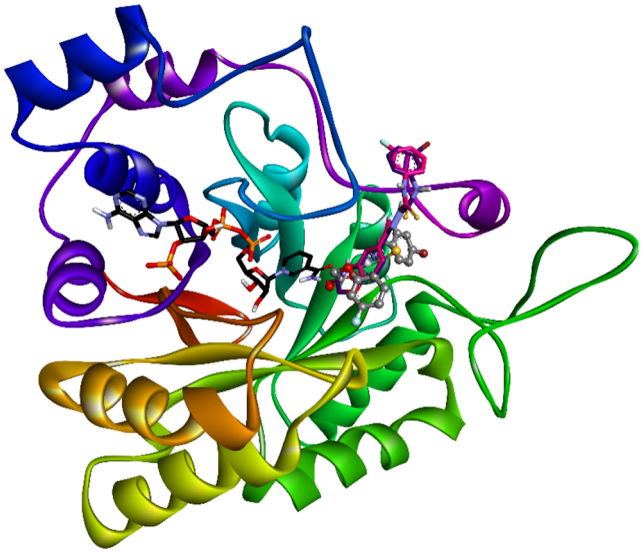

Fig. 6. Overlap of docked ALR2 inhibitors **3l** (pink) and **3b** (purple) with the co-crystallized inhibitor LDT320 (in ball and stick representation). NADPH is represented in black colored sticks.

250–252 °C, IR υ (cm^{-1}): 1181(C═S), 1587 (C═N), 1686 (C═O), 3214,3285 (N−H), ^{1}H NMR (DMSO-d_6) δ ppm; 2.29 (s, 3H, CH_3), 4.58 (s, 2H, O-CH_2-CO), 6.93 (d, 1H, benzoxazin Ar-H, J = 8.0 Hz), 7.17 (m, 1H, Ar-H), 7.34 (m, 2H, Ar-H), 7.41 (d, 1H, benzoxazin Ar-H, J = 8.0 Hz), 7.54 (dd 2H, Ar-H, J = 1.0 Hz, 8.0 Hz), 7.59 (dd, 1H, benzoxazin Ar-H, J = 1.0 Hz, 2.5 Hz), 9.87 (s,1H, NH-CS), 10.62 (s,1H, NH-N), 10.69 (s, 1H, NH-CO); ^{13}C NMR δ ppm; 14.90, 67.30, 114.49, 116.38, 122.65, 125.61, 125.77, 127.54, 128.72,132.27, 139.51, 144.99, 148.91, 165.05,177.13. Anal calcd for $C_{17}H_{16}N_4O_2S$ (340.40); C, 59.98; H, 4.74; N, 16.46; Found C, 59.76; H, 4.54; N, 16.34.

4.2.1.2. ***N-(3-Bromophenyl)-2-(1-(3-oxo-3,4-dihydro-2H-benzo[b][1,4]oxazin-6-yl)ethylidene) Hydrazinecarbothioamide (3b)***. Yield 78%, m.p. 274–276 °C , IR υ_{max} (cm^{-1}): 1181 (C═S), 1579 (C═N), 1699 (C═O), 3232,3303 (N−H), ^{1}H NMR (DMSO-d_6) δ ppm; 2.27 (s, 3H, CH_3), 4.58 (s, 2H, O-CH_2-CO), 6.93 (d, 1H, benzoxazin Ar-H, J = 8 Hz), 7.29–7.34(m, 3H, Ar-H), 7.40 (d, 1H, benzoxazin Ar-H , J = 0.8 Hz), 7.60–7.63 (m, 1H, Ar-H), 7.93 (t, 1H, benzoxazin Ar-H , J = 0.8 Hz, 2 Hz), 9.96 (s,1H, NH-CS), 10.70 (s,1H, NH-N), 10.74 (s, 1H, NH-CO); ^{13}C NMR δ ppm; 15.01, 67.31, 114.68, 116.39, 121.12, 122.70, 124.57, 127.52, 127.79, 128.28, 130.49, 132.19, 141.19, 145.04, 149.56, 165.07, 177.04. Anal calcd for $C_{17}H_{15}BrN_4O_2S$ (419.30); C, 48.70; H, 3.61, N, 13.36; Found; C, 48.35; H, 3.52, N, 13.86.

4.2.1.3. ***N-(3-Chlorophenyl)-2-(1-(3-oxo-3,4-dihydro-2H-benzo[b][1,4]oxazin-6-yl)ethylidene) Hydrazinecarbothioamide (3c)***. Yield 80%, m.p. 290–292 °C , IR υ_{max} (cm^{-1}): 1182 (C═S), 1590 (C═N), 1686 (C═O), 3266,3285 (N−H), ^{1}H NMR (DMSO-d_6) δ ppm; 2.29 (s, 3H, CH_3), 4.59 (s, 2H, O-CH_2-CO), 6.97 (d, 1H, benzoxazin Ar-H, J = 8 Hz), 7.32–7.35 (m, 3H, Ar-H), 7.40 (d, 1H, bezoxazin Ar-H, J = 0.8 Hz), 7.54–7.57 (m, 1H, Ar-H), 7.81 (t, 1H, benzoxazin Ar-H , J = 0.8 Hz, 2 Hz), 9.96 (s,1H, NH-CS), 10.70 (s,1H, NH-N), 10.74 (s, 1H, NH-CO); ^{13}C NMR δ ppm; 15.01, 67.28, 114.63, 116.37, 116.59, 122.21, 124.93, 127.60, 130.22, 132.19, 132.78, 141.05, 145.05, 149.57, 165.07, 165.16, 177.03. Anal calcd for $C_{17}H_{15}ClN_4O_2S$ (374.84); C, 54.47; H, 4.03, N, 14.95; Found; C, 54.35; H, 4.14, N, 14.35.

4.2.1.4. ***N-Benzyl-2-(1-(3-oxo-3,4-dihydro-2H-benzo[b][1,4]oxazin-6-yl)ethylidene)hydrazine Carbothioamide (3d)***. Yield 72%, m.p. 230–232 °C, IR υ_{max} (cm^{-1}): 1180 (C═S), 1562 (C═N), 1683 (C═O), 3127,3235 (N−H), ^{1}H NMR (DMSO-d_6) δ ppm; 2.23 (s, 3H, CH_3), 4.56 (s, 2H, O-CH_2-CO), 4.82 (s, 2H, Ph-CH_2), 6.91 (d, 1H, benzoxazin Ar-H, J = 8 Hz), 7.26–7.30(m, 6H, Ar-H and bezoxazin Ar-H), 7.56 (d, 1H, bezoxazin Ar-H , J = 0.8 Hz, 2 Hz), 8.86 (s,1H, NH-CS), 10.32 (s,1H, NH-N), 10.66 (s, 1H, NH-CO); ^{13}C NMR δ ppm; 14.80, 47.22, 67.30, 114.74, 116.44, 122.27, 127.25, 127.46, 127.70, 128.71, 128.73, 132.61, 139.88, 144.77, 148.36, 165.04, 179.00. Anal calcd for $C_{18}H_{18}N_4O_2S$ (354.43); C, 61.00; H, 5.12; N, 15.81; Found; C, 61.30; H, 5.25; N, 15.31

4.2.1.5. ***N-(2-Morpholinoethyl)-2-(1-(3-oxo-3,4-dihydro-2H-benzo[b][1,4]oxazin-6-yl)ethylidene)hydrazinecarbothioamide (3e)***. Yield 76%, m.p. 228–230 °C , IR υ_{max} (cm^{-1}): 1281 (C═S), 1528 (C═N), 1686 (C═O), 3285,3357 (N−H), ^{1}H NMR (DMSO-d_6) δ ppm; 2.29 (s, 3H, CH_3), 2.42 (m, 8H, CH_2-N), 3.50–3.65 (m, 4H, CH_2-O),4.58 (s, 2H, O-CH_2-CO), 6.91 (dd, 1H, benzoxazin Ar-H, J = 0.8 Hz, 8 Hz), 7.23(dd, 1H, benzoxazin Ar-H , J = 0.8 Hz, 2 Hz), 7.50 (dd, 1H, benzoxazin Ar-H , J = 2 Hz, 8 Hz), 8.35 (s,1H, NH-CS), 10.32 (s,1H, NH-N), 10.66 (s, 1H, NH-CO); ^{13}C NMR δ ppm; 14.70, 53.63, 56.87, 66.82, 67.30, 114.67, 116.46, 121.79, 127.53, 132.68, 144.75, 147.74, 165.07, 178.22. Anal calcd for $C_{17}H_{23}N_5O_3S$ (377.46); C, 54.09; H, 6.14; N, 18.55 Found;C, 54.30; H, 6.24; N, 18.25.

4.2.1.6. ***N-(2-Chlorobenzyl)-2-(1-(3-oxo-3,4-dihydro-2H-benzo[b][1,4]oxazin-6-yl)ethylidene) Hydrazinecarbothioamide (3f)***. Yield 70%, m.p. 278–280 °C , IR υ_{max} (cm^{-1}): 1181 (C═S), 1518 (C═N),

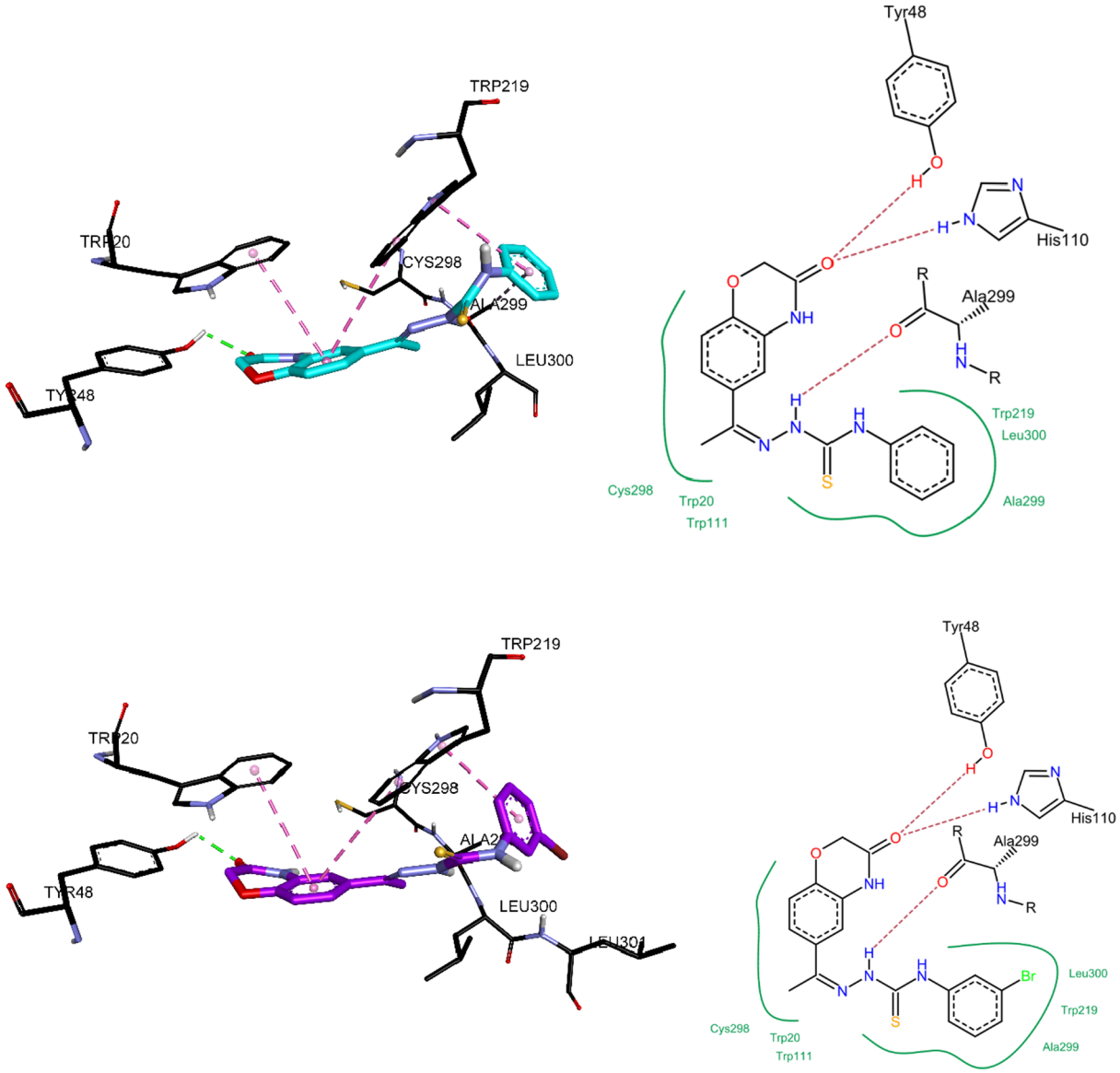

Fig. 7. 3D and 2D docked conformations of most active ALR2 inhibitors **3l** (pink), and **3b** (purple).

1692 (C═O), 3255,3380 (N—H), ^{1}H NMR (DMSO-d_6) δ ppm; 2.25 (s, 3H, CH_3), 4.56 (s, 2H, O-CH_2-CO), 4.87 (s, 2H, Ph-CH_2), 6.92 (d, 1H, benzoxazin Ar-H , J = 8 Hz,), 7.21–7.29(m, 4H, Ar-H), 7.41 (d, 1H, benzoxazin Ar-H, J = 8 Hz),7.57 (d, 1H, benzoxazin Ar-H , J = 8 Hz), 8.86 (brs,1H, NH-CS), 10.48 (s,1H, NH-N), 10.68 (s, 1H, NH-CO); ^{13}C NMR δ ppm; 14.84, 45.17, 67.31, 114.78, 116.46, 122.30, 127.47, 127.57, 128.57,128.87, 129.55, 132.00, 132.57, 136.78, 144.83, 148.59, 165.06, 179.39. Anal calcd for $C_{18}H_{17}ClN_4O_2S$ (388.87); C, 55.59; H, 4.41, N, 14.41; Found; C, 55.20; H, 4.12, N, 14.83.

4.2.1.7. ***N-(Naphthalen-1-yl)-2-(1-(3-oxo-3,4-dihydro-2H-benzo[b][1,4]oxazin-6-yl)ethylidene) Hydrazinecarbothioamide (3 g)***. Yield 91%, m.p. 278–80 °C , IR υ_{max} (cm^{-1}): 1185 (C═S), 1520 (C═N), 1682 (C═O), 3315 (N—H), ^{1}H NMR (DMSO-d_6) δ ppm; 2.33 (s, 3H, CH_3), 4.55 (s, 2H, O-CH_2-CO), 6.90 (d, 1H, benzoxazin Ar-H, J = 8.8 Hz), 7.42 (d, 1H, benzoxazin Ar-H, J = 2.4 Hz), 7.49–7.52 (m, 2H, benzoxazin Ar-H), 7.67 (dd, 1H, Ar-H, J = 2 Hz), 7.79–7.87 (m, 2H, Ar-H), 7.93–7.95 (m, 1H, Ar-H), 10.12 (s,1H, NH-CS), 10.53 (s,1H, NH-N), 10.70 (s, 1H, NH-CO); ^{13}C NMR δ ppm; 14.85, 67.30, 114.78, 116.38, 122.67, 125.99, 126.59, 126.73, 126.79, 127.43, 130.91, 132.42, 134.22, 136.11, 144.92, 148.70, 165.03, 179.22. Anal calcd for $C_{21}H_{18}N_4O_2S$ (390.12); C, 64.60; H, 4.65; N, 14.35; Found; C, 64.66; H, 4.71, N, 14.41.

4.2.1.8. ***N-(3-Methoxyphenyl)-2-(1-(3-oxo-3,4-dihydro-2H-benzo[b][1,4]oxazin-6-yl)ethylidene)hydrazinecarbothioamide (3 h)***. Yield 84%, m.p. 236–238 °C , IR υ_{max} (cm^{-1}): 1169 (C═S), 1596 (C═N), 1703 (C═O), 3302 (N—H), ^{1}H NMR (DMSO-d_6) δ ppm; 2.29 (s, 3H, CH_3), 3.72 (s, 3H, OCH_3), 4.58 (s, 2H, O-CH_2-CO), 6.75 (m, 1H, Ar-H), 6.93(d, 1H, benzoxazin Ar-H, J = 8 Hz), 7.17–7.24 (m, 2H, Ar-H), 7.36–7.41(m, 2H, benzoxazin Ar-H), 7.52 (d, 1H, Ar-H, J = 8 Hz), 9.83 (s,1H, NH-CS), 10.64 (s,1H, NH-N), 10.70 (s, 1H, NH-CO); ^{13}C NMR δ ppm; 14.94, 55.69, 67.30, 110.94, 111.12, 114.48, 116.37, 117.53, 122.66, 127.57, 129.44, 132.24, 140.59, 145.01, 149.03, 159.61, 165.05, 176.83. Anal calcd for $C_{18}H_{18}N_4O_3S$ (370.43); C, 58.36; H, 4.90; N, 15.12; Found; C, 58.28; H, 4.45; N, 15.20.

4.2.1.9. ***2-(1-(3-Oxo-3,4-dihydro-2H-benzo[b][1,4]oxazin-6-yl) ethylidene)-N-(p-tolyl) hydrazine carbothioamide (3i)***. Yield 88%, m.p. 294–296 °C , IR υ_{max} (cm^{-1}): 1190 (C═S), 1510 (C═N), 1666 (C═O), 3254,3281 (N—H), ^{1}H NMR (DMSO-d_6) δ ppm; 2.26 (s, 3H, CH_3), 2.28 (s, 3H, CH_3), 4.57 (s, 2H, O-CH_2-CO), 6.93 (d, 1H,

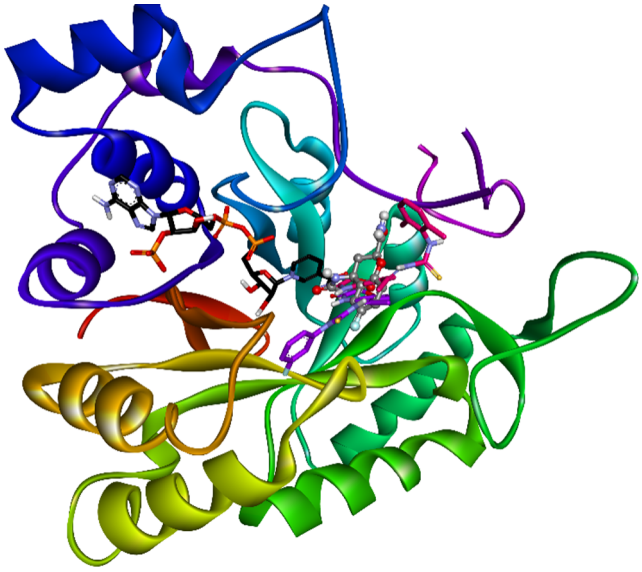

Fig. 8. Overlap of docked ALR1 inhibitors **3q** (pink) and **3l** (purple) with the co-crystallized inhibitor FID2401 (in ball and stick representation). NADP is represented in black colored sticks.

benzoxazin Ar-H, J = 8.4 Hz), 7.08–7.14 (m, 2H, Ar-H), 7.40 (d, 1H, benzoxazin Ar-H, J = 2.4 Hz), 7.45 (dd, 1H, benzoxazin Ar-H, J = 8.4 Hz, 2 Hz), 7.53 (dd, 1H, benzoxazin Ar-H, J = 2.4 Hz, 2 Hz), 9.78 (s,1H, NH-CS), 10.54 (s,1H, NH-N), 10.67 (s, 1H, NH-CO); ^{13}C NMR δ ppm; 14.85, 21.10, 67.29, 114.47, 116.38, 122.63, 125.60, 125.60, 127.52, 129.11, 129.16, 132.30, 134.99, 136.93, 144.96, 148.76, 165.06, 177.17. Anal calcd for $C_{18}H_{18}N_4O_2S$ (354.12); C, 61.00; H, 5.12; N,15.81; Found; C, 61.05; H, 5.20; N,15.90.

4.2.1.10. ***N-Cyclohexyl-2-(1-(3-oxo-3,4-dihydro-2H-benzo[b][1,4] oxazin-6-yl)ethylidene) hydrazinecarbothioamide (3j)***. Yield 80%, m.p. 234–236 °C , IR υ_{max} (cm^{-1}): 1198 (C=S), 1580 (C=N), 1690 (C=O), 3133, 3232, 3335 (N−H), ^{1}H NMR (DMSO-d_6) δ ppm; 2.20 (s, 3H, CH_3), 3.31–3.39 (m,11*H*, cyclohexyl ring), 4.57 (s, 2H, O-CH_2-CO), 6.92 (d, 1H, benzoxazin Ar-H, J = 8 Hz), 7.29 (d, 1H, benzoxazin Ar-H , J = 8 Hz), 7.37 (dd, 1H, benzoxazin Ar-H , J = 0.8 Hz, 2 Hz), 9.3 (s,1H, NH-CS), 10.19 (s,1H, NH-N), 10.78 (s, 1H, NH-CO); ^{13}C NMR δ ppm; 14.71, 25.09, 25.27, 25.62, 32.10, 32.46, 52.83, 67.27, 114.00, 116.43, 122.30, 127.62, 132.48, 144.83, 147.90, 165.15, 177.10. Anal calcd for $C_{17}H_{22}N_4O_2S$ (346.45); C, 58.94; H, 6.40; N, 16.17; Found; C, 58.38; H, 6.58; N, 16.40.

4.2.1.11. ***N-(2-Fluorophenyl)-2-(1-(3-oxo-3,4-dihydro-2H-benzo[b] [1,4]oxazin-6-yl)ethylidene) hydrazinecarbothioamide (3 k)***. Yield 70%, m.p. 314–316 °C , IR υ_{max} (cm^{-1}): 1212 (C=S), 1597 (C=N), 1673 (C=O), 3085, 3271 (N−H), ^{1}H NMR (DMSO-d_6) δ ppm; 2.17 (s, 3H, CH_3), 4.55 (s, 2H, O-CH_2-CO), 6.90 (d, 1H, benzoxazin Ar-H , J = 8 Hz), 7.25(d, 1H, benzoxazin Ar-H, J = 8 Hz), 7.35 (d, 1H, benzoxazin Ar-H, J = 0.8 Hz, 2 Hz), 7.40–7.52 (m, 4H, Ar-H), 10.24 (s,1H, NH-CS,), 10.35 (s,1H, NH-N), 10.70 (s, 1H, NH-CO); ^{13}C NMR δ ppm; 13.87, 21.32, 22.21, 67.23, 67.31, 113.93, 116.26, 116.42, 121.65, 122.13, 127.64, 133.11, 144.51, 146.58, 165.14, 165.15, 173.28 Anal calcd for $C_{17}H_{15}FN_4O_2S$ (358.39); C, 56.97; H, 4.22, N, 15.63; Found; C, 56.58; H, 4.40, N, 15.54.

4.2.1.12. ***N-(3-Fluorophenyl)-2-(1-(3-oxo-3,4-dihydro-2H-benzo[b] [1,4]oxazin-6-yl)ethylidene) hydrazinecarbothioamide (3 l)***. Yield 87%, m.p. 254–256 °C , IR υ_{max} (cm^{-1}): 1190 (C=S), 1594 (C=N), 1684 (C=O), 3235,3384 (N−H), ^{1}H NMR (DMSO-d_6) δ ppm; 2.29 (s, 3H, CH_3), 4.56 (s, 2H, O-CH_2-CO), 6.92 (d, 1H, benzoxazin Ar-H, J = 8 Hz), 7.35–7.45 (m, 3H, Ar-H), 7.52 (dd, 1H, benzoxazin Ar-H, J = 2 Hz, 8 Hz),7.65–7.72 (m, 2H, benzoxazin Ar-H& Ar-H), 9.92 (s,1H, NH-CS), 10.52 (s,1H, NH-N), 10.56 (s, 1H, NH-CO); ^{13}C NMR δ ppm; 15.01, 67.30, 112.24, 114.57, 116.39, 121.07, 122.71, 127.55, 130.21, 132.17 141.32, 145.04, 149.50, 160.88, 163.29, 165.05, 176.88. Anal calcd for $C_{17}H_{15}FN_4O_2S$ (358.39); C, 56.97; H, 4.22, N, 15.63; Found; C, 56.49; H, 4.30, N, 15.49.

4.2.1.13. ***N-(4-Nitrophenyl)-2-(1-(3-oxo-3,4-dihydro-2H-benzo[b] [1,4]oxazin-6-yl)ethylidene) hydrazinecarbothioamide (3 m)***. Yield 81%, m.p. 278–280 °C , IR υ_{max} (cm^{-1}): 1178 (C=S), 1544 (C=N), 1700 (C=O), 3276,3343 (N−H), ^{1}H NMR (DMSO-d_6) δ ppm; 2.31 (s, 3H, CH_3), 4.58 (s, 2H, O-CH_2-CO), 6.94 (d, 1H, benzoxazin Ar-H, J = 8 Hz), 7.41 (d, 1H, benzoxazin Ar-H , J = 8 Hz), 8.04–8.07 (m, 2H, Ar-H), 8.19–8.21 (m,3H, benzoxazin Ar-H & Ar-H) 10.27 (s,1H, NH-CS), 10.74 (s,1H, NH-N), 11.00 (s, 1H, NH-CO); ^{13}C NMR δ ppm; 15.20, 67.29, 114.67, 116.43, 122.81, 124.19, 124.21, 124.22, 124.41, 127.55, 132.06, 143.81, 145.17, 145.88, 150.54, 165.06, 176.60. Anal calcd for $C_{17}H_{15}N_5O_4S$ (385.40); C, 52.98; H, 3.92; N, 18.17; Found; C, 52.90; H, 3.86; N, 18.10.

4.2.1.14. ***2-(1-(3-Oxo-3,4-dihydro-2H-benzo[b][1,4]oxazin-6-yl) ethylidene)hydrazine carbo thioamide (3n)*** *[31]*. Yield 84%, m.p. 292–294 °C, IR υ_{max} (cm^{-1}): 1204 (C=S), 1581 (C=N), 1675 (C=O), 3307,3485 (N−H), ^{1}H NMR (DMSO-d_6) δ ppm; 2.20 (s, 3H, CH_3), 4.56 (s, 2H, O-CH_2-CO), 6.89 (d, 1H, benzoxazin Ar-H , J = 8 Hz), 7.33 (d, 1H, benzoxazin Ar-H, J = 8 Hz,), 7.45–7.48(m, 1H, benzoxazin Ar-H), 8.29 (brs,1H, H-NH-CS), 10.23 (s,1H, NH-N), 10.57 (s, 1H, NH-CO); ^{13}C NMR δ ppm; 14.50, 67.30, 114.36, 116.36, 122.31, 127.47, 132.51, 144.78, 147.84, 165.02, 179.34. Anal calcd for $C_{11}H_{12}N_4O_2S$ (264.30); C, 49.99; H, 4.58; N, 21.20; Found; C, 49.89; H, 4.49; N, 21.26.

4.2.1.15. ***N-(4-Fluorophenyl)-2-(1-(3-oxo-3,4-dihydro-2H-benzo[b] [1,4]oxazin-6-yl)ethylidene) hydrazinecarbothioamide (3o)***. Yield 85%, m.p. 280–282 °C , IR υ_{max} (cm^{-1}): 1207 (C=S), 1543 (C=N), 1698 (C=O), 3228,3306 (N−H), ^{1}H NMR (DMSO-d_6) δ ppm; 2.28 (s, 3H, CH_3), 4.57 (s, 2H, O-CH_2-CO), 6.92 (d, 1H, benzoxazin Ar-H, J = 8 Hz), 7.14–7.19 (m, 2H, Ar-H), 7.40 (d, 1H, benzoxazin Ar-H, J = 8 Hz),7.53–7.58 (m, 3H, benzoxazin Ar-H & Ar-H), 9.68 (s,1H, NH-CS), 10.63 (s,1H, NH-N), 10.67 (s, 1H, NH-CO); ^{13}C NMR δ ppm; 14.91, 67.31, 114.65,115.17, 115.43, 116.37, 122.64, 127.50, 128.16, 132.28, 135.0.94, 144.97, 149.07, 158.91, 161.31, 165.04, 177.60. Anal calcd for $C_{17}H_{15}FN_4O_2S$ (358.39); C, 56.97; H, 4.22,N, 15.63; Found; C, 56.82, H, 4.32, N, 15.75.

4.2.1.16. ***N-(2,4-Dichlorophenyl)-2-(1-(3-oxo-3,4-dihydro-2H-benzo [b][1,4]oxazin-6-yl) ethylidene)hydrazinecarbothioamide (3p)***. Yield 82%, m.p. 266–268 °C , IR υ_{max} (cm^{-1}): 1196 (C=S), 1527 (C=N), 1681 (C=O), 3314 (N−H), ^{1}H NMR (DMSO-d_6) δ ppm; 2.30 (s, 3H, CH_3), 4.57 (s, 2H, O-CH_2-CO), 6.93 (d, 1H, benzoxazin Ar-H, J = 8 Hz), 7.34 (d, 1H, benzoxazin Ar-H, J = 8 Hz), 7.42 (dd, 1H, benzoxazin Ar-H, J = 0.8 Hz, 2 Hz),7.55–7.58 (m, 1H, Ar-H), 7.68 (d, 1H, Ar-H, J = 2 Hz), 7.89 (d, 1H, Ar-H, J = 8 Hz), 9.92 (s,1H, NH-CS), 10.71 (s,1H, NH-N), 10.92 (s, 1H, NH-CO); ^{13}C NMR δ ppm; 15.12, 67.30, 114.69, 116.51, 122.57, 127.56, 127.73, 129.22, 130.33, 131.18, 132.24, 136.09 145.09, 149.62 165.07. Anal calcd for $C_{17}H_{14}Cl_2N_4O_2S$ (409.29); C, 49.89; H, 3.45, N, 13.69; Found; C, 49.80; H, 3.52, N, 13.56.

4.2.1.17. ***N-(2,6-Dimethylphenyl)-2-(1-(3-oxo-3,4-dihydro-2H-benzo[b][1,4]oxazin-6-yl) ethylidene)hydrazinecarbothioamide (3q)***. Yield 88%, m.p. 276–278 °C , IR υ_{max} (cm^{-1}): 1192 (C=S), 1507 (C=N), 1676 (C=O), 3250,3285 (N−H), ^{1}H NMR (DMSO-d_6) δ ppm; 2.32 (s, 6H, 2 × CH_3), 2.29 (s, 3H, CH_3), 4.56 (s, 2H, O-CH_2-CO), 6.91 (d, 1H, benzoxazin Ar-H , J = 8 Hz), 7.0.05–7.07 (m, 3H, Ar-H), 7.37 (d, 1H, benzoxazin Ar-H, J = 8 Hz),7.65 (dd, 1H, benzoxazin Ar-H, J = 0.8 Hz, 2 Hz), 9.51 (s,1H, NH-CS), 10.50 (s,1H, NH-N), 10.56 (s,

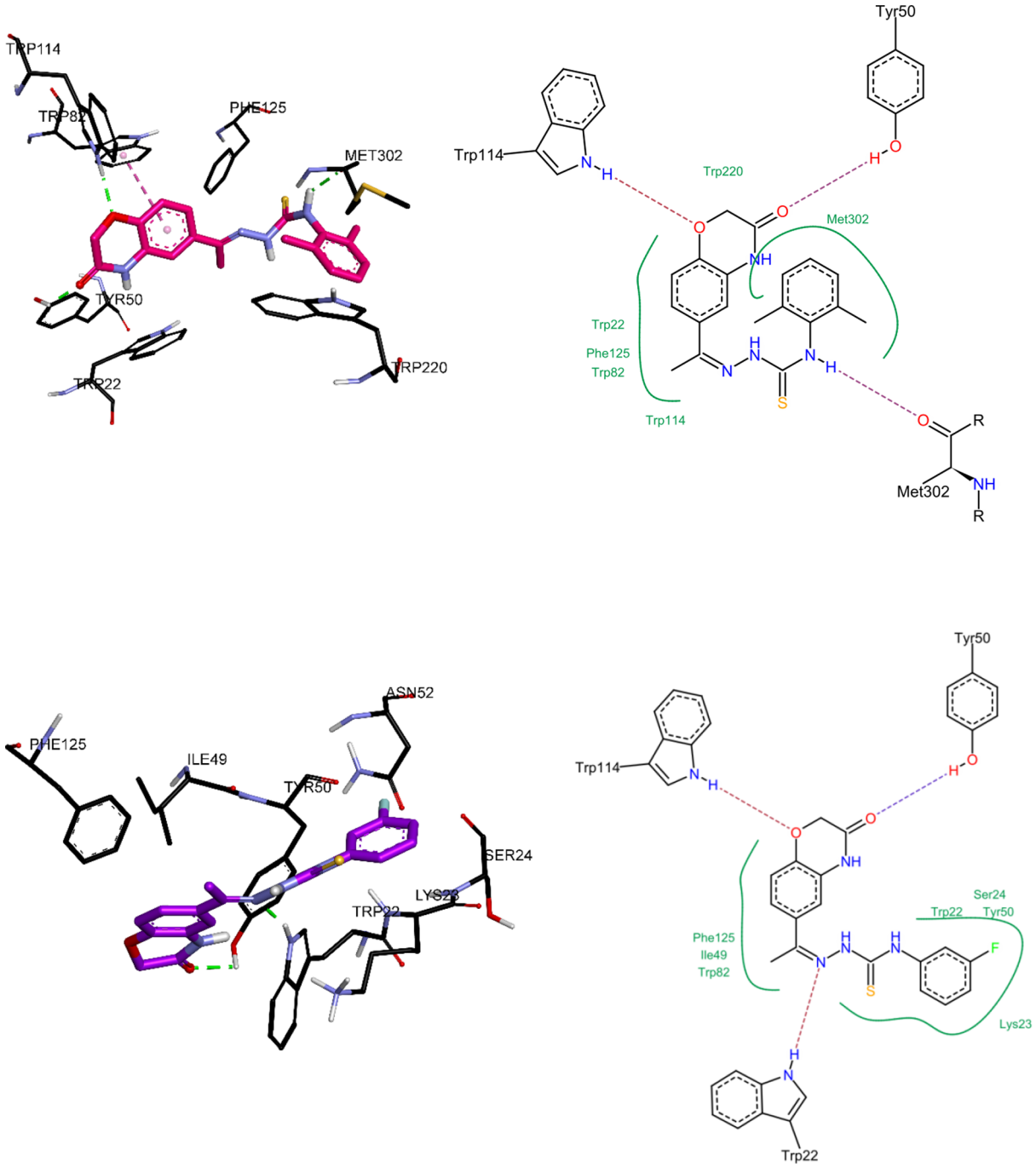

Fig. 9. 3D and 2D docked conformations of most active ALR1 inhibitors **3q** (pink), and **3l** (purple).

1H, NH-CO); ^{13}C NMR δ ppm; 14.61, 18.62, 67.32, 114.77, 116.33, 122.56, 127.38, 127.46, 128.13, 132.49, 136.90, 137.73, 144.82, 147.75, 165.04, 178.22. Anal calcd for $C_{19}H_{20}N_4O_2S$ (368.45); C, 61.94; H, 5.47; N,15.21; Found; C, 61.85; H, 5.42; N,15.18.

4.2.1.18. ***2-(1-(3-Oxo-3,4-dihydro-2H-benzo[b][1,4]oxazin-6-yl) ethylidene)-N-(p-tolyl) hydrazine carbothioamide (3r)***. Yield 90%, m.p. 256–258 °C , IR υ_{max} (cm^{-1}): 1187 (C═S), 1519 (C═N), 1661 (C═O), 3263, 3292 (N–H), ^{1}H NMR (DMSO-d_6) δ ppm; 2.20 (s, 3H, CH_3), 2.28 (s, 3H, CH_3), 4.56 (s, 2H, O-CH_2-CO), 6.91 (d, 1H, benzoxazin Ar-H, J = 8.8 Hz), 7.15–7.25 (m, 3H, Ar-H), 7.33–7.36 (m, 3H, Ar-H), 7.38 (d, 1H, benzoxazin Ar-H, J = 2.4 Hz), 7.61 (dd, 1H, benzoxazin Ar-H, J = 8.4 Hz, 2.4 Hz), 9.70 (s,1H, NH-CS), 10.59 (s,1H, NH-N), 10.62 (s, 1H, NH-CO); ^{13}C NMR δ ppm; 14.76, 18.35, 67.31, 114.60, 116.37, 122.56, 126.44, 127.08, 127.47, 128.71, 130.61, 132.39, 135.37, 138.48, 144.89, 148.22, 165.03, 177.99. Anal calcd for $C_{18}H_{18}N_4O_2S$ (354.12); C, 61.00; H, 5.12; N,15.81; Found; C, 61.19; H, 5.22; N,15.76.

Acknowledgment

J. Iqbal is thankful to the Organization for the Prohibition of Chemical Weapons (OPCW), The Hague, The Netherlands and Higher Education Commission of Pakistan through Project No. 20-3733/ NRPU/R&D/14/520 for the financial support. Z. Shafiq is thankful to Bahauddin Zakariya University (BZU), Multan for providing financial support to Ph.D. student.

Appendix A. Supplementary material

Supplementary data to this article can be found online at https://doi.org/10.1016/j.bioorg.2018.12.006.

References

[1] Y. Shi, F.B. Hu, The Lancet 383 (2014) 1947–1948.
[2] D.R. Whiting, L. Guariguata, C. Weil, J. Shaw, Diab. Res. Clin. Pract. 94 (2011) 311–321.
[3] P. Alexiou, K. Pegklidou, M. Chatzopoulou, I. Nicolaou, V.J. Demopoulos, Curr. Med. Chem. 16 (2009) 734–752.
[4] P. Alexiou, V.J. Demopoulos, J. Med. Chem. 53 (2010) 7756–7766.
[5] Q. Mohamed, T.Y. Wong, Exp. Opin. Emerg. Drugs 13 (2008) 675–694.
[6] R. Ottanà, R. Maccari, M. Giglio, A. Del Corso, M. Cappiello, U. Mura, S. Cosconati, L. Marinelli, E. Novellino, S. Sartini, Eur. J. Med. Chem. 46 (2011) 2797–2806.
[7] V.J. Demopoulos, N. Zaher, C. Zika, C. Anagnostou, E. Mamadou, P. Alexiou, I. Nicolaou, Drug Des. Rev. 2 (2005) 293–304.
[8] P.F. Kador, W.G. Robison Jr, J.H. Kinoshita, Annu. Rev. Pharmacol. Toxicol. 25 (1985) 691–714.
[9] K.V. Ramana, S.K. Srivastava, Int. J. Biochem. Cell Biol. 42 (2010) 17–20.
[10] R. Ramasamy, I.J. Goldberg, Circ. Res. 106 (2010) 1449–1458.
[11] T. Petrova, H. Steuber, I. Hazemann, A. Cousido-Siah, A. Mitschler, R. Chung, M. Oka, G. Klebe, O. El-Kabbani, A. Joachimiak, J. Med. Chem. 48 (2005) 5659–5665.
[12] A. Saeed, Y. Tehseen, H. Rafique, N. Furtmann, J. Bajorath, U. Flörke, J. Iqbal, Med. Chem. Comm. 5 (2014) 1371–1380.
[13] H.A. Bhatti, Y. Tehseen, K. Maryam, M. Uroos, B.S. Siddiqui, A. Hameed, J. Iqbal, Bioorg. Chem. 75 (2017) 62–70.
[14] A. Ibrar, Y. Tehseen, I. Khan, A. Hameed, A. Saeed, N. Furtmann, J. Bajorath, J. Iqbal, Bioorg. Chem. 68 (2016) 177–186.
[15] X. Hao, Z. Han, Y. Li, C. Li, X. Wang, X. Zhang, Q. Yang, B. Ma, C. Zhu, Bioorg. Med. Chem. Lett. 27 (2017) 887–892.
[16] S. Miyamoto, Exp. Opin. Ther. Pat. 12 (2002) 621–631.
[17] K. Šturm, L. Levstik, V.J. Demopoulos, A. Kristl, Eur. J. Pharm. Sci. 28 (2006) 128–133.
[18] M. Chatzopoulou, P. Alexiou, E. Kotsampasakou, V.J. Demopoulos, Exp. Opin. Ther. Pat. 22 (2012) 1303–1323.
[19] A. Hameed, K.M. Khan, S.T. Zehra, R. Ahmed, Z. Shafiq, S.M. Bakht, M. Yaqub, M. Hussain, A.d.l.V. de León, N. Furtmann, J. Bajorath, H.A. Shad, M.N. Tahir, J. Iqbal, Bioorg. Chem. 61 (2015) 51–57.
[20] A. Hameed, M. Yaqub, M. Hussain, A. Hameed, M. Ashraf, H. Asghar, M.M. Naseer, K. Mahmood, M. Muddassar, M.N. Tahir, Z. Shafiq, RSC Adv. 6 (2016) 63886–63894.
[21] A. Hameed, Z. Shafiq, M. Yaqub, M. Hussain, M.A. Hussain, M. Afzal, M.N. Tahir, M.M. Naseer, New J. Chem. 39 (2015) 9351–9357.
[22] M. Taha, H. Ullah, L.M.R. Al Muqarrabun, M.N. Khan, F. Rahim, N. Ahmat, M.T. Javid, M. Ali, K.M. Khan, Bioorg. Med. Chem. 26 (2018) 152–160.
[23] M. Hayat, K.M. Khan, S. Saeed, U. Salar, M. Khan, T. Baig, A. Ahmad, S. Parveen, M. Taha, Lett. Drug Des. Discov. 15 (2018) 1057–1067.
[24] B. Ali, K.M. Khan, U. Salar, S. Hussain, M. Ashraf, M. Riaz, A. Wadood, M. Taha, S. Perveen, Bioorg. Chem. 79 (2018) 363–371.
[25] B. Bano, K.M. Khan, A. Lodhi, U. Salar, F. Begum, M. Ali, M. Taha, S. Perveen, Bioorg. Chem. 80 (2018) 129–144.
[26] S. Iqbal, M. Saleem, M.K. Azim, M. Taha, U. Salar, K.M. Khan, S. Perveen, M.I. Choudhary, Bioorg. Chem. 72 (2017) 89–101.
[27] E. Howard, R. Sanishvili, R. Cachau, A. Mitschler, B. Chevrier, P. Barth, V. Lamour, M. Van Zandt, E. Sibley, C. Bon, Prot.: Struct., Funct., Bioinf. 55 (2004) 792–804.
[28] O. El-Kabbani, N.C. Green, G. Lin, M. Carson, S. Narayana, K. Moore, T. Flynn, L. DeLucas, Acta. Cryst. D 50 (1994) 859–868.
[29] V. Carbone, H.-T. Zhao, R. Chung, S. Endo, A. Hara, O. El-Kabbani, Bioorg. Med. Chem. 17 (2009) 1244–1250.
[30] J.-T. Zhou, C.-L. Li, L.-H. Tan, Y.-F. Xu, Y.-H. Liu, Z.-Z. Mo, Y.-X. Dou, R. Su, Z.-R. Su, P. Huang, PLoS One 12 (2017) e0168944.
[31] G.J. Reddy, K.S. Rao, Heterocycl. Commun. 12 (2006) 473–476.